Cite this: DOI: 10.1039/c0xx00000x

www.rsc.org/xxxxxx

ARTICLE TYPE

Structural snapshots of the SCR reaction mechanism on Cu-SSZ-13

Tobias Günter,[a] Hudson W.P. Carvalho,[a] Dmitry E. Doronkin,[a,b] Thomas Sheppard,[a] Pieter Glatzel,[c] Andrew J. Atkins,[d] Julian Rudolph,[e] Christoph R. Jacob,[d,e] Maria Casapu,[a] Jan-Dierk Grunwaldt*[a,b]

Received (in XXX, XXX) Xth XXXXXXXXX 20XX, Accepted Xth XXXXXXXXX 20XX

DOI: 10.1039/b000000x

The structure of copper sites in Cu-SSZ-13 during NH_3-SCR was unravelled by a combination of novel operando X-ray spectroscopic techniques. Strong adsorption of NH_3 on Cu, its reaction with weakly adsorbed NO from the gas phase, and slow re-oxidation of Cu(I) were proven. Thereby the SCR reaction mechanism is significantly different to Fe-ZSM-5.

Selective catalytic reduction of NO_x by ammonia (NH_3-SCR) over iron and copper based catalysts is presently the predominant way to remove hazardous NO_x from automotive exhaust gases.[1] In particular the chabazite-based catalysts Cu-SSZ-13 and Cu-SAPO-34 have recently attracted strong interest due to their outstanding performance and hydrothermal stability.[2] Although Cu-SSZ-13 has already been commercialized, the reaction mechanism and the active site are still strongly debated.[3] Typically, single Cu^{2+} sites are located close to a six- or eight-member ring (6MR or 8MR).[4] They are mobile, dynamically change their structure,[4c] and less active Cu dimers can be formed at intermediate temperatures.[5] This structural variation inevitably requires operando studies.

In situ X-ray absorption spectroscopy (XAS) has uncovered high redox dynamics of Cu sites in the chabazite framework, particularly promoted during the standard SCR process.[4b, 6] This redox behavior, which is similar to Fe-zeolites, originates from the reaction of NO and NH_3.[7] The reduction of Cu^{2+} sites was observed also in an NH_3 containing stream.[7-8] Nevertheless, the nature of adsorbed species and the sequence of reaction steps are still controversial. For large-pore zeolites the reaction between gaseous or oxidatively adsorbed NO and adsorbed NH_3 has been proposed.[6a, 9] Oxidative adsorption of NO_x together with stronger non-dissociative adsorption of NH_3 on Cu sites has been reported on both Cu-SAPO-34 and Cu-SSZ-13.[10] Furthermore, formation of nitrosyl groups NO^+ has been found by IR spectroscopy.[11] The interaction of Cu^{2+} sites in Cu-SAPO-34 with both NO and NH_3 was further evidenced by in situ EPR.[12] With respect to the influence of other gaseous species, a positive effect of water for the SCR reaction has been reported, although it strongly inhibits NO oxidation.[3, 13] However, most of the studies that can evidence the interaction between the adsorbates and copper were not performed under operating conditions, which appears particularly important as previously demonstrated by Ribeiro et al.[4b, 14] Recent investigations have shown that combined synchrotron-based hard-X-ray photon-in/photon-out techniques[15] allow probing in situ not only the oxidation state and the coordination sphere but also the nature of the ligands.[8, 14b]

Here we report on the use of High Energy Resolution Fluorescence Detected XAS (HERFD-XAS) and Valence-to-Core X-ray Emission Spectroscopy (V2C XES) at the Cu K-edge under NH_3-SCR operating conditions to shed light on the standard SCR mechanism over Cu-SSZ-13. For this purpose, we prepared a well-defined Cu-SSZ-13 catalyst and studied the structure at relevant SCR conditions and systematically under 12 defined reference conditions to understand the influence of each species and their interactions. The spectra were further interpreted using reference compounds and density-functional theory (DFT) calculations. In addition, we compare the results to our recent HERFD-XAS/XES study over Fe-ZSM-5.[14b]

The 1.2wt% Cu-SSZ-13 catalyst was prepared by ion-exchange with copper acetate (ESI) resulting in a Si:Al-ratio of 16:1 and Cu:Al = 0.2:1. EXAFS data analysis shows mostly isolated 4-fold coordinated Cu^{2+} sites with a Cu-O bond distance around 1.96 Å (ESI, Fig. S3). This is in line with literature, where isolated sites are observed for the used ion exchange level, possibly close to 8 membered rings under the applied reaction conditions.[16] This catalyst sample demonstrated typical SCR activity with a seagull shaped light-off curve (ESI, Fig. S2). Next, the catalyst was tested in an operando fixed-bed quartz capillary microreactor cell.[17] These experiments were performed with a sieve fraction of 100 - 200 µm (ESI) to avoid mass transfer limitations,[17] which can strongly influence SCR activity over Cu-zeolites.[18] Fig. 1 shows that conversion of NO in the operando cell was close to the results obtained in the laboratory fixed-bed reactor, underlining its suitability. Water enhanced the performance in both cases, being slightly more pronounced at low temperatures, in line with previous studies on Cu-zeolite catalysts.[19,13]

[a,b] *Institute for Chemical Technology and Polymer Chemistry (ITCP) & Institute of Catalysis Research and Technology (IKFT), Karlsruhe Institute of Technology, D-76131 Karlsruhe, E-mail: grunwaldt@kit.edu*
[c] *European Synchrotron Radiation Facility, 6 rue Jules Horowitz, BP 220, F-38043 Grenoble Cedex, France*
[d] *Center for Functional Nanostructures and Institute of Physical Chemistry, Karlsruhe Institute of Technology, Wolfgang-Gaede-Str. 1a, D-76131 Karlsruhe, Germany*
[e] *Institute of Physical and Theoretical Chemistry, TU Braunschweig, Hans-Sommer-Str. 10, D-38106 Braunschweig, Germany*

† Electronic Supplementary Information (ESI) available: Experimental details, Synthesis, Catalytic performance, EXAFS, DFT calculations. See DOI: 10.1039/b000000x/

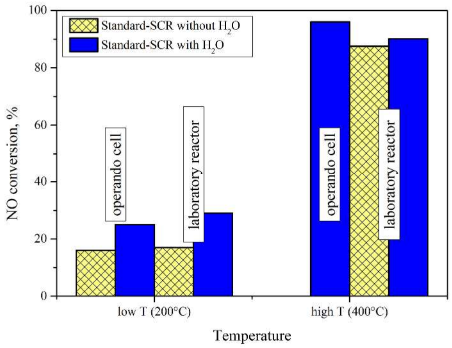

Fig. 1. Catalytic activity of 1.2wt% Cu-SSZ-13 measured in the lab fixed-bed reactor and the operando cell at the beamline. Conditions: 1000 ppm NO, 1000 ppm NH_3, 10% O_2, 0 - 1.5% H_2O, N_2 balance (laboratory), He balance (beamline); GHSV = 200 000 h^{-1}.

The results obtained with XAS / XES are first described separately and afterwards correlated to obtain a coherent picture. The numbering of the conditions was chosen to present spectral differences and is not according to the experimental order. Before each experiment, the sample was treated to reach its initial state.

HERFD-XANES spectra were collected during NO and NH_3 oxidation, and under standard SCR with or without water (Fig. 2). At first glance, major changes of the XANES profiles are visible for conditions involving NH_3. However, important variations could be observed for all investigated conditions. The HERFD-XANES spectrum of the untreated sample in synthetic air at room temperature (condition 1) contains features typical for Cu-SSZ-13:[8] a pre-edge feature **A** at 8977.5 eV (1s → 3d transition in Cu^{2+}),[20] a small shoulder **B** at 8982.7 eV (1s → 4p transition of two-coordinated Cu^+ sites)[6a] and a second shoulder **C** at 8986.5 eV (Cu^{2+} 1s → 4p transition with ligand to metal charge transfer (LMCT, shakedown))[8, 21]. A similar profile was recorded at 200 °C in the presence of water (cond. 4) which corresponds to hydrated Cu^{2+} sites. Dehydration by pretreatment at 550 °C (cond. 2) led to a slightly higher intensity of the pre-edge and of the features **B** and **C**. The white-line showed a sharper main feature **E** around 8997 eV accompanied by a shoulder **D** at 8993 eV, indicating a slight difference in the coordination sphere.[22] Analysis of the pre-edge region indicates a majority of Cu^{2+} sites present under these conditions. The removal of oxygen and H_2O (cond. 3) led to a decrease of **A,** suggesting an autoreduction, also evidenced by integration of the background-subtracted pre-edge feature (about 60% of the Cu^{2+} sites are reduced under He).

With respect to the reactant gases, NO addition mainly affected features **B** and **C**. Thus dosing only NO + He (cond. 7) yielded the highest intensity of **C** but a diminishment of feature **B** in comparison to cond. 2 (O_2/He). Both features **B** and **C** decrease when NO and O_2 are dosed over the catalyst bed, indicating the complete absence of Cu^+ species. This could be caused by oxidation of the remaining Cu^+ sites by traces of NO_2. Moreover, shoulder **C** almost vanishes on addition of H_2O. These results preclude the reduction of the Cu sites by NO at 200 °C. As reduction of the Cu^{2+} sites is expected during the SCR-reaction, the adsorption of NO on Cu^+ species was verified after reduction at 550 °C in 5% H_2/He (cond. 13). Note that the corresponding HERFD-XANES shows a shoulder around 8981 eV probably due to overreduction to Cu^0.[22-23]

The second group of spectra, which involve NH_3 (cond. 8 - 12), exhibit an intense feature **B** suggested to originate from linear coordination of the Cu sites.[8, 21, 24] The highest intensity of feature **B** was observed in NH_3-He (cond. 9) combined with an almost complete disappearance of the pre-edge feature **A**, which strongly suggests reduction of Cu^{2+} species. The addition of NH_3 (cond. 8, 10) to the oxidizing atmosphere also led to reduced intensity in the 1s → 3d pre-edge region, combined with a shift of this feature by 0.2 eV to higher energies, which is possibly due to structural distortion or higher ligand field splitting.[25] The presence of H_2O and O_2 in the gas mixture led to a stepwise decrease of feature **B**

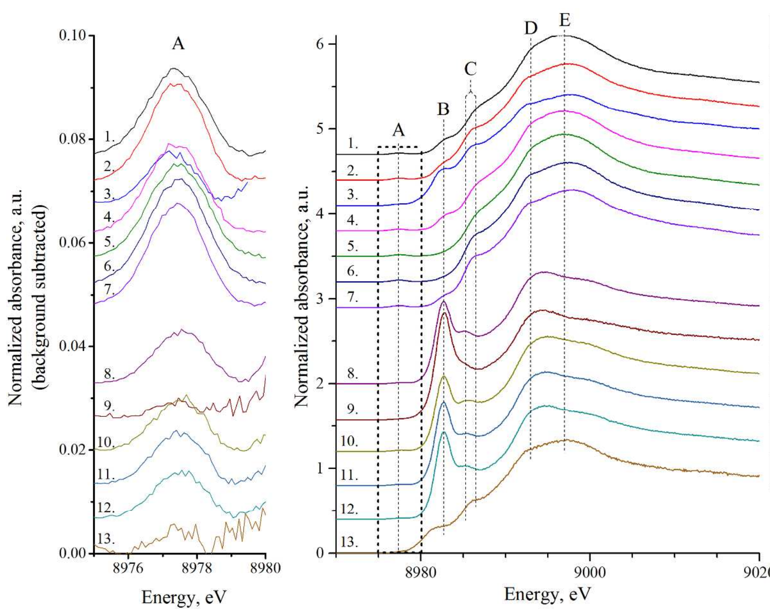

#	Gas composition	fraction Cu^{2+}
1.	O_2 + He, RT	90% Cu^{2+}
2.	O_2 + He	95% Cu^{2+}
3.	He	40% Cu^{2+}
4.	O_2 + He + H_2O	90% Cu^{2+}
5.	NO + O_2 + He + H_2O	100% Cu^{2+}
6.	NO + O_2 + He	100% Cu^{2+}
7.	NO + He	100% Cu^{2+}
8.	NH_3 + O_2 + He	50% Cu^{2+}
9.	NH_3 + He	n.a.
10.	NH_3 + O_2 + He + H_2O	45% Cu^{2+}
11.	NH_3 + NO + O_2 + He + H_2O	45% Cu^{2+}
12.	NH_3 + NO + O_2 + He	40% Cu^{2+}
13.	NO + He, prereduced	n.a.

Fig. 2. Cu K-edge HERFD-XANES (middle) and pre-edge region (left) of Cu-SSZ-13 during NH_3-SCR and under model gas mixtures at 200 °C (exact gas composition and temperature given in the ESI, Table S2). Estimation of Cu^{2+} amount (±10%) relative to all Cu in the sample based on the integral of the background-subtracted pre-edge peak (at 8977.4 eV) taking the spectra of conditions 1,2,4-7 as Cu^{2+} reference (details, cf. ESI).

(higher coordination, more oxidized). As no NH_3 oxidation is observed at this temperature, a reaction can be excluded, suggesting a competitive (or three-fold) adsorption of NH_3 and H_2O at the Cu-sites as also observed by NH_3-TPD (Fig. S16) and shown for other Cu-systems.[26]

Dosing the standard SCR gas mixture NO + NH_3 + O_2 (cond. 12) at 18% NO_x conversion resulted in a spectrum similar to NH_3 + O_2 (cond. 8), only a little decrease of the main feature **B** was observed. The more realistic gas mixture with water (cond. 11) led to a spectrum similar to NH_3 + O_2 + H_2O (cond. 10).

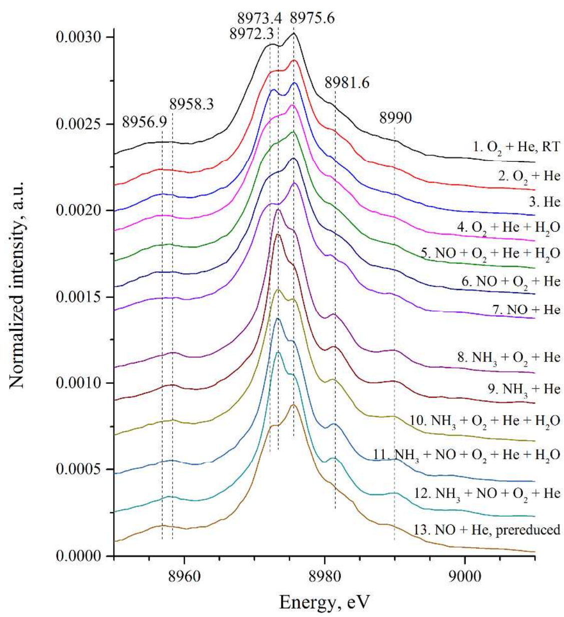

Fig. 3. XES spectra of Cu-SSZ-13 catalyst during NH_3-SCR and under related model gas mixtures at 200 °C (exact composition and temperature given in the ESI, Table S2).

Next, we focused on the X-ray emission spectra (Fig. 3). Similarly to the HERFD-XANES results, the spectra can be divided into two very similar groups showing the same features, i.e. catalyst without NH_3 in the feed (cond. 1-7, 13) and catalyst with NH_3 in the feed (cond. 8-12, including SCR and NH_3 oxidation conditions). The differences between those groups are the following: (a) Appearance of a second peak upon NH_3 addition in the Kβ" region at 8958.3 eV which is seen either as broadening of peak 8956.9 eV (both peaks have similar intensity in cond. 9, 10, 11) or a shift of this peak (dominating over the peak at 8956.9 eV in cond. 8 and 12). These features are similar to those reported during in-situ adsorption of NH_3 on Cu-SSZ-13 by Giordanino et al.[8] and can be attributed to an N atom in the coordination sphere of Cu, i.e. direct adsorption of NH_3. DFT-calculations on the influence of the ligand environment on the XES spectra support such an assignment (Fig. S10). No feature stemming from ammonia adsorbed via hydroxyl groups was detected for copper. This is in contrast to the Fe-O^+H-NH_x moiety observed for Fe-ZSM-5.[14b] (b) A peak at 8972.3 eV in the $K\beta_{2,5}$ region which is shifted to 8973.4 eV and becomes more intense upon removal of reactants with only NH_3/He remaining, (c) Increased intensity of features at 8981.6 and 8990.0 eV after adsorption of NH_3, probably due to a change in geometry of the Cu complex. The changes named above stem only from interaction with ammonia but not from the change of Cu oxidation state which is verified by exp. 13 (vs. exp. 7) where no significant changes are observed after NO-adsorption on pre-reduced Cu.

Mainly minor changes in relative intensity of the $K\beta_{2,5}$ peaks were observed for the group of spectra recorded in NH_3-free atmosphere. The addition of NO (in He) caused broadening or diminishment of the Kβ" features compared to the dehydrated catalyst in He. However, no clear peak at 8958.3 eV from an N atom was noted upon adsorption of NO (cond. 7). In the presence of O_2 and H_2O, the peak at 8956.9 eV showed basically no change upon NO addition. This indicates a strong inhibition effect particularly due to H_2O (ESI, Fig. S12, ref.[13]) and points to weak adsorption of NO probably via the O atom as isonitrosyl, accompanied by small changes in the coordination environment of Cu sites.

Strikingly different from the case of NO and NH_3 adsorption over Fe-ZSM-5 is the absence of a Kβ" peak at low energy which we ascribed to a positively polarized/triple coordinated oxygen atom with NO bound via Fe-O.[14b] This difference in adsorption of NO on Fe- and Cu-zeolites is substantial and may explain the debated differences in SCR performance and also in NO oxidation activity of those zeolites.[27] Indeed, NO adsorbs via an additional O atom as a nitrite-like intermediate on an Fe site and then can be readily desorbed as NO_2, whereas in the case of Cu NO seems to be adsorbed as a nitroso-group and, hence, can desorb easily again as NO or react with adsorbed NH_3. DRIFTS has recently evidenced NO^+ on Cu-CHA catalysts.[4c, 13]

In summary, we observed strong NH_3 adsorption on Cu sites under all conditions involving ammonia, the intensity of the NH_3-related XANES features was lower for the feeds containing water. Such behavior with water can be caused either by inhibition of NH_3 adsorption or by an increased Cu^+ reoxidation rate[28]. A positive influence of water on the SCR rate was evidenced earlier[5, 19, 29] and also found in the current study. Concerning NO, its adsorption is supported by the change of shape of the Kβ" peak and also of the HERFD-XANES spectra (cond. 7 vs. 3). However, in the presence of O_2 and/or H_2O (cond. 5 and 6) only the relative intensities of peaks in the $K\beta_{2,5}$ region changed and the NO adsorption must be weak. Those small changes are completely indiscernible behind the features arising from NH_3 and therefore in the current state of work we assume that either NO is weakly adsorbed, or rapidly reacts from the gas phase with adsorbed ammonia/amino groups.

The proposed mechanism depicted in Scheme 1 only partially supports the mechanism suggested by Gao et al.[3] since the formation of NH_3-Cu^+-NO^+ could not be unambiguously demonstrated. Thus, the presented data indicate that during standard SCR, NH_3 adsorbs on a Cu^{2+} site via direct coordination. Next, NO may adsorb on the same site via O and react with NH_3 or directly react from the gas phase as suggested by several previous studies.[6a, 9, 30] Both paths could circumvent the blockage of the Cu sites at low temperatures by NH_3, which is in contrast to the Fe-ZSM-5 case, where the strong NH_3-adsorption (Fig. S15) additionally inhibits the reoxidation. NO might be activated by interaction with NH_3 or Cu^{2+}. The decomposition of the formed nitrosoamide[3] intermediate may be facilitated by the presence of water (Fig. 1) via an ammonium nitrite formation and subsequent thermal decomposition (not shown) or because it stabilizes the resulting undercoordinated Cu^+. As a result of SCR and its electron transfer processes, a reduced Cu^+ site with low coordination number is found, in accordance with the spatially-resolved XAS study of Cu-SAPO-34,[7] which is then oxidized by O_2 and H_2O to Cu^{2+} as a slow and rate-limiting step and stabilized as Cu^{2+}-OH^{4c}. Although suggested in literature, no proof for the participation of NOx in this reaction step was found. In contrast to Fe-ZSM-5, water has a beneficial effect as the Cu^+ is significantly less coordinated than the resulting Fe^{2+}. In addition, for Fe-ZSM-5-catalyst coordination of NO and NH_3 via oxygen has been suggested to either Fe or V, which could not be found for Cu in Cu-SSZ-13.

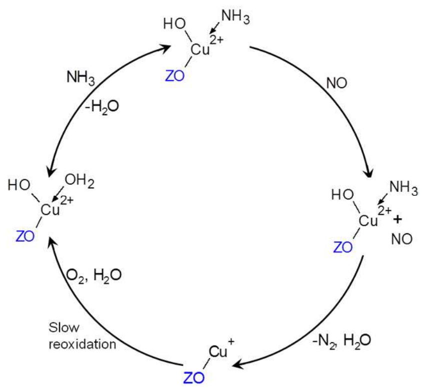

Scheme 1. Role of copper in Cu-SSZ-13 suggested by *operando* XES and XAS during NH_3-SCR. Possible additional water / ammonia ligands are left out for clarity. ZO stands for zeolite cation-exchange site.

By combining operando HERFD-XAS and V2C XES we could provide important new insight into the structure of copper and its interaction with NH_3 and NO during standard SCR. A significant difference in the intermediate species during SCR over Fe-ZSM-5 and Cu-SSZ-13 was found. This difference could explain the higher activity of Cu-zeolites at low temperatures and the absence of an NH_3 inhibition effect. Furthermore, it could be correlated with the different NO oxidation behavior of the Fe- and Cu-zeolites. In future, it would be valuable to extend these studies to vanadia SCR catalysts and exploit the same approach of combining HERFD-XANES, XES, and EXAFS including DFT-calculations for simulating the spectra to other reactions.

This work has been supported by KIT, the Federal Ministry of Education and Research (BMBF, projects 05K10VKB and 05K13VK2) and DBU (T. Günter). We thank ESRF for providing the beamtime at the ID26 beamline and financial support at ESRF and C. Lapras for the technical support. We are also grateful to E. Japke for the assistance during XES measurements and T. Bergfeldt (IAM-AWP, KIT) for elemental analysis.

Notes and references

1 (a) I. Nova and E. Tronconi, *Urea-SCR Technology for deNOx After Treatment of Diesel Exhausts*, Springer, New York, 2014; (b) U. Deka, I. Lezcano-Gonzalez, B. M. Weckhuysen and A. M. Beale, *ACS Catalysis*, 2013, **3**, 413.

2 (a) P. G. Blakeman, E. M. Burkholder, H.-Y. Chen, J. E. Collier, J. M. Fedeyko, H. Jobson and R. R. Rajaram, *Catal. Today*, 2014, **231**, 56; (b) S. J. Schmieg, S. H. Oh, C. H. Kim, D. B. Brown, J. H. Lee, C. H. F. Peden and D. H. Kim, *Catal. Today*, 2012, **184**, 252.

3 F. Gao, J. Kwak, J. Szanyi and C. H. F. Peden, *Top. Catal.*, 2013, 1.

4 (a) F. Gao, E. D. Walter, E. M. Karp, J. Luo, R. G. Tonkyn, J. H. Kwak, J. Szanyi and C. H. F. Peden, *J. Catal.*, 2013, **300**, 20; (b) S. A. Bates, A. A. Verma, C. Paolucci, A. A. Parekh, T. Anggara, A. Yezerets, W. F. Schneider, J. T. Miller, W. N. Delgass and F. H. Ribeiro, *J. Catal.*, 2014, **312**, 87; (c) R. Zhang, J.-S. McEwen, M. Kollár, F. Gao, Y. Wang, J. Szanyi and C. H. F. Peden, *ACS Catalysis*, 2014, **4**, 4093.

5 F. Gao, E. D. Walter, M. Kollar, Y. Wang, J. Szanyi and C. H. F. Peden, *J. Catal.*, 2014, **319**, 1.

6 (a) C. Paolucci, A. A. Verma, S. A. Bates, V. F. Kispersky, J. T. Miller, R. Gounder, W. N. Delgass, F. H. Ribeiro and W. F. Schneider, *Angew. Chem., Int. Ed.*, 2014, **53**, 11828; (b) J. S. McEwen, T. Anggara, W. F. Schneider, V. F. Kispersky, J. T. Miller, W. N. Delgass and F. H. Ribeiro, *Catal. Today*, 2012, **184**, 129.

7 D. E. Doronkin, M. Casapu, T. Günter, O. Müller, R. Frahm and J.-D. Grunwaldt, *J. Phys. Chem. C*, 2014, **118**, 10204.

8 F. Giordanino, E. Borfecchia, K. A. Lomachenko, A. Lazzarini, G. Agostini, E. Gallo, A. V. Soldatov, P. Beato, S. Bordiga and C. Lamberti, *J. Phys. Chem. Lett.*, 2014, **5**, 1552.

9 H. Sjövall, E. Fridell, R. Blint and L. Olsson, *Top. Catal.*, 2007, **42-43**, 113.

10 (a) L. Shi, T. Yu, X. Wang, J. Wang and M. Shen, *Acta Phys.-Chim. Sin.*, 2013, **29**, 1550; (b) H. Zhu, J. H. Kwak, C. H. F. Peden and J. Szanyi, *Catal. Today*, 2013, **205**, 16.

11 J. Szanyi, J. H. Kwak, H. Zhu and C. H. F. Peden, *Phys. Chem. Chem. Phys.*, 2013, **15**, 2368.

12 T. Yu, T. Hao, D. Fan, J. Wang, M. Shen and W. Li, *J. Phys. Chem. C*, 2014, **118**, 6565.

13 M. P. Ruggeri, I. Nova, E. Tronconi, J. A. Pihl, T. J. Toops and W. P. Partridge, *Appl. Catal., B*, 2015, **166–167**, 181.

14 (a) V. F. Kispersky, A. J. Kropf, F. H. Ribeiro and J. T. Miller, *Phys. Chem. Chem. Phys.*, 2012, **14**, 2229; (b) A. Boubnov, H. W. P. Carvalho, D. E. Doronkin, T. Günter, E. Gallo, A. J. Atkins, C. R. Jacob and J.-D. Grunwaldt, *J. Am. Chem. Soc.*, 2014, **136**, 13006.

15 (a) P. Glatzel and U. Bergmann, *Coord. Chem. Rev.*, 2005, **249**, 65; (b) N. Lee, T. Petrenko, U. Bergmann, F. Neese and S. DeBeer, *J. Am. Chem. Soc.*, 2010, **132**, 9715; (c) M. Bauer, *Phys. Chem. Chem. Phys.*, 2014, **16**, 13827.

16 E. Borfecchia, K. A. Lomachenko, F. Giordanino, H. Falsig, P. Beato, A. V. Soldatov, S. Bordiga and C. Lamberti, *Chem. Sci.*, 2015, **6**, 548.

17 J. D. Grunwaldt, M. Caravati, S. Hannemann and A. Baiker, *Phys. Chem. Chem. Phys.*, 2004, **6**, 3037.

18 P. S. Metkar, V. Balakotaiah and M. P. Harold, *Chem. Eng. Sci.*, 2011, **66**, 5192.

19 H. Sjövall, L. Olsson, E. Fridell and R. J. Blint, *Appl. Catal., B*, 2006, **64**, 180.

20 E. M. C. Alayon, M. Nachtegaal, E. Kleymenov and J. A. van Bokhoven, *Micropor. Mesopor. Mat.*, 2013, **166**, 131.

21 L. S. Kau, D. J. Spira-Solomon, J. E. Penner-Hahn, K. O. Hodgson and E. I. Solomon, *J. Am. Chem. Soc.*, 1987, **109**, 6433.

22 N. B. Castagnola, A. J. Kropf and C. L. Marshall, *Appl. Catal., A*, 2005, **290**, 110.

23 M. K. Neylon, C. L. Marshall and A. J. Kropf, *J. Am. Chem. Soc.*, 2002, **124**, 5457.

24 R. A. Himes, G. Y. Park, A. N. Barry, N. J. Blackburn and K. D. Karlin, *J. Am. Chem. Soc.*, 2007, **129**, 5352.

25 K.-I. Shimizu, H. Maeshima, H. Yoshida, A. Satsuma and T. Hattori, *Phys. Chem. Chem. Phys.*, 2001, **3**, 862.

26 (a) P. Kappen, J.-D. Grunwaldt, B. S. Hammershøi, L. Tröger and B. S. Clausen, *J. Catal.*, 2001, **198**, 56; (b) R. Kumashiro, Y. Kuroda and M. Nagao, *J. Phys. Chem. B*, 1998, **103**, 89.

27 M. Ruggeri, I. Nova and E. Tronconi, *Top. Catal.*, 2013, **56**, 109.

28 G. T. Palomino, P. Fisicaro, S. Bordiga, A. Zecchina, E. Giamello and C. Lamberti, *J. Phys. Chem. B*, 2000, **104**, 4064.

29 (a) J. A. Sullivan, J. Cunningham, M. A. Morris and K. Keneavey, *Appl. Catal., B*, 1995, **7**, 137; (b) A. V. Salker and W. Weisweiler, *Appl. Catal., A*, 2000, **203**, 221.

30 L. Xu, R. W. McCabe and R. H. Hammerle, *Appl. Catal., B*, 2002, **39**, 51.